MATERION

WHITE PAPER

A Comparison of Electroplated Gold Flash Palladium-Nickel and Clad Gold Alloy Capped Palladium-Silver

materion.com/iON-connector

WHITE PAPER

ABSTRACT

This study examines the properties of both electroplated gold flash palladium-nickel (GFPdNi) and clad WE#1 capped palladium-silver (WE#1/PdAg), which is a Materion iON connector material. The electrical resistivities were measured in order to understand contact resistance differences. Electrical stability during and after environmental and mechanical tests was evaluated. Environmental tests included thermal aging at elevated temperature and Battelle flowing mixed gas exposure. Mechanical tests included formability, sliding wear and fretting. Key attributes which were measured and reported included, electrical resistivity, hardness, contact resistance, porosity level, coefficient of friction during sliding wear, and fretting cycles to failure. It was found that GFPdNi demonstrated lower electrical resistivity, higher hardness, lower initial contact resistance, lower coefficient of friction and greater durability during sliding wear. WE#1/PdAg demonstrated acceptably low initial coefficient of friction, greater electrical stability during thermal aging and Battelle FMG exposure, better formability, and greater resistance to fretting wear.

INTRODUCTION

Palladium based contact materials have been used successfully in telecommunications, computer and automotive dry circuit applications. Wrought materials have been based upon palladium-silver alloys with-a nominal composition of 60 weight per-cent Pd, 40 weight per-cent Ag. EJectroplated materials have included pure Pd but the predominant material is now a palladium-nickel co-deposit with a nominal composition of 80 weight per-cent Pd, 20 weight per-cent Ni.

Pd alloys and co-deposits demonstrate acceptable electrical resistivity, high hardness, low initial contact resistance, low coefficient of friction, and low porosity. However, palladium is not as noble as gold. Pd is directly attacked by nitric acid and develops $PdCl_2 \cdot 2H_20$ when exposed to chlorine at high humidity [1]. Further, insulating surface films readily form during exposure to flowing mixed gas environments [2,3]. PdNi alloys and co-deposits oxidize when aged in air at temperatures above 125°C [4]. Finally, deleterious frictional polymers may form when mated Pd surfaces are subjected to micro-motion in the presence of organic vapors [5].

The nobility of the contact surface may be increased by coating Pd alloy or co-deposit with a thin, 0.05 to 0.25 micro-meter, layer of gold or gold alloy. This thin surface layer attenuates chemical attack and oxidation, acts as a boundary layer lubricant during sliding, and may promote the formation of beneficial frictional polymers during fretting [6-8].

The purpose of this study was to compare electroplated gold flash palladium-nickel to a wrought contact system consisting of a thin layer of WE#1 (69Au25Ag6Pt) over palladium-silver.

Bulk properties of the individual materials such as hardness, formability, electrical resistivity and, thermal and chemical stability are reported. The contact material systems were evaluated for porosity, chemical and thermal stability, sliding wear, and fretting behavior. Methods of analysis included direct measurement of porosity, contact resistance measurement before and after aging at elevated temperature in air, contact resistance measurement before and after exposure to flowing mixed gas environments, coefficient of friction during rider-on-flat sliding wear, and contact resistance measurement during fretting.

MATERIAL SYSTEMS

The electroplated material system consisted of 0.1 µ-meter nominal cobalt hardened gold (AuCo) as a surface layer, 1.0 1-1-meter 80 palladium-20 nickel as an intermediate layer, and 2.0 µ-meter sulfamate nickel as an underlayer. This system will be referred to as GFPdNi throughout the balance of this paper.

The wrought clad-inlay material system consisted of 0.25 µ-meter of WE#1 as a surface layer, 0.50 µ-meter of 60 palladium-40 silver as an intermediate layer, and 8 µ-meter of N02270 as an underlayer. This system will be referred to as WE#1/PdAg throughout the balance of this paper.

The spring material was 0.25 mm thick copper alloy CI7410 heat treated to ½ HT temper designation. This particular material-temper combination was selected because of strength and ductility requirements imposed by the following test conditions.

TESTING AND EVALUATION TECHNIQUES

Hardness tests were performed with a micro-indentation hardness tester using a Vickers indentor. Both 50 and 100 gram loads were used. Five readings were obtained for each sample at each load and averaged.

The electrical resistivity of the wrought materials was determined using a Thomson bridge to measure the resistance of a 0.65 mm x 25 mm x 300 mm samples and calculating the resistivity using the relationship

$$\rho = R \cdot \frac{A}{L} \qquad \text{Equation 1}$$

Where, ρ is the electrical resistivity, R is the measured resistance, A is the cross-sectional area and, L is the sample length.

A Hewlett-Packard 4328A four wire milli-ohmmeter was used to measure initial contact resistance and on the thermally aged and Battelle Class II FMG exposure samples. A minimum of 5 and up to 1oo measurements were obtained for each test condition. During measuring, maximum current was limited to 15 mA at 10 mΩ full scale. Upward adjustment of the full scale to measure resistances in excess of 10 mΩ reduces the applied current Maximum voltage for the case .of incorrect range setting was limited to 20 mV; maximum voltage was 200 μV for proper range setting. Contact· resistance measurements were obtained using a 50 gram load.

Formability was evaluated using 90° V-blocks machined to specific radii. The formed surface was subsequently exposed to nitric acid vapors as specified in ASTM· B-735 to evaluate the surface continuity.

Porosity was determined by two techniques. The first method was single step paper electrography per ASTM B-741.

The second method was direct pore count after exposure to Battelle Class II FMG for 48 hours.

Thermal exposure was accomplished by placing samples of the contact materials in a laboratory oven operated at 150°C ± 5°C. Duration ranged from one to 20 weeks.

Exposure to Battelle Class II flowing mixed gas (FMG) was accomplished at Battelle Memorial Institute, Columbus, OH. Samples were exposed from 48 to 240 hours.

The wear test apparatus consisted of a moveable table and a fixed balance beam. Both the table and the beam were mounted on an air slide. Contact loads were achieved with standard weights. A load cell was attached to the beam to measure the coefficient of friction (COF). The test parameters were 10. Hz and 6 mm wipe distance. Contact forces of 0.5,1.0, 5.0 and 10.0 N were used. Both contact members were ultrasonically cleaned in isopropyl alcohol prior to each test run. No additional lubricant was applied to the mating surfaces.

Fretting test were conducted at the Advanced Interconnection Laboratory at New Mexico State University, Las Cruces, NM. The fretting machine uses phased electrodynamic drivers to move a low-inertia oscillating tube. Fretting displacements down to 1.0 micro-meter are monitored by a LASER displacement instrument [9]. The machine was operated in the constant displacement mode. The contact force was 0.5 N.·Experimental conditions included, 20 and 50 micro-meter displacements, 10 and 100 mA current flow and, 40% and 80% relative humidity. Both contact members were solvent cleaned prior to each test run. No additional lubricant was applied to the mating surfaces.

RESULTS AND DISCUSSION

HARDNESS AND ELECTRICAL RESISTIVITY

Table 1. Contains the hardness and electrical resistivities for Au, WE#1, 60Pd40Ag, 80Pd20Ni as well as the hardness and contact resistance of GFPdNi and WE#1/PdAg. Hardness values for cobalt hardened gold and electroplated 80Pd20Ni were taken from the literature [4]. Contact resistance measurements were obtained using gold probes and a 50 gram load. Although the resistivity of 60Pd40Ag is significantly higher than 80Pd20Ni, the contact resistance of WE#1/PdAg is nearly equivalent to GFPdNi. If surface films are absent, the contact resistance is simply the constriction resistance. Constriction resistance is a function of

contact area and resistivity. The contact area can be calculated by dividing the hardness in kg/mm^2 by the contact load in kg. The formula for constriction resistance, R_c, is,

$$R_c = 9 \cdot \rho \sqrt{\left(\frac{H}{W}\right)} \qquad \text{Equation 2}$$

where, ρ is the resistivity, H is the hardness of the softest component which in this case is the probe, and W the contact 'toad. For Gi=PDNI PdNi, assuming 70 kg/mm^2 for the gold probe hardness and 0.05 kg (50 gr.) contact load, the expected contact resistance would be

$$9 \times 0.0000053 \times \sqrt{(70/.05)} = 0.0018\Omega$$

For WE#1/PdAg,

$$9 \times 0.0000154 \times \sqrt{(70/.05)} = 0.0052\Omega$$

TABLE 1: HARDNESS, RESISTIVITY, AND CONTACT RESISTANCE VALUES FOR THE MATERIALS EVALUATED IN THIS STUDY

MATERIAL	HARNESS HV 50, KG/MM^2	RESISTIVITY μΩ-CM	CONTACT RESISTANCE, MΩ
Pure Gold	60-80	2.35	0.8
Cobalt Gold	120-200	4.7-5.9	2.6-2.8
WE#1	120-140	15.4	3.1-3.4
60Pd40Ag	165-210	42.0	5.0-6.5
80Pd20Ni	350-500	21.2	3.1-5.8
WE#1/PdAg	180	-	2.7-3.9
GFPdNi	330	-	2.3-6.4

The predicted contact resistance for GFPdNi was lower than measured, while that for WE#1/PdAg was higher than measured. For multi-layer contact systems, the measured hardness value is typically closer to that of the intermediate layer. The surface layer is too thin to support the load and the intermediate layer serves as an anvil providing support. The difference between measured and calculated R_c was due to the intermediate layer hardness.

POROSITY

Table II contains the results of porosity measurements on WE#1/PdAg and GFPDNI PdNi surfaces.

TABLE II: RESULTS OF POROSITY TESTS. UNITS ARE PORES/CM^2

MATERIAL	ASTM B-741	CLASS II FMG
WE#1/PdAg	2-5	3-5
GFPdNi	0-2	21-34

The disparate results for GFPdNi were unexpected given that electroplated 80Pd20Ni has been reported to be pore free at thicknesses of 1.0 μmeter or greater. While GFPdNi demonstrated very low porosity when subjected to a standard porosity test, in this case, electrographic, the level of porosity increased by more than an order of magnitude when subjected to Battelle Class II FMG. These results are consistent with recent findings by Abbott and Antler [10]. The difference in behavior can be explained with an understanding of the fundamental reasons for the two tests. Porosity tests are usually employed as · process control tools and are designed to check the integrity of the coating without attacking the coating. The electrographic porosity test results in Table II corroborate the low porosity characteristics of PdNi.

Lees has examined GFPdNi surfaces using $HN0_3$ vapors per ASTM B-735 [11]. This test does result in the attack of the PdNi layer and objections have been raised to this practice.

The reason for selecting this test method has not been to evaluate the integrity of the coating. Rather, because the corrosion products of PdNi, Ni and Cu characteristic and contrasting colors - PdNi products are black, Ni white and Cu light aqua - the test can be used to determine the relative porosity of the individual layers. For GFPdNi, typical pore densities for .1 µmeter AuCo have been reported at 200-350 pores/cm^2; PdNi 0-6 pores/cm^2. A similar evaluation of WE#1/PdAg yielded pore densities for WE#1 of 35 -70 pores/cm^2 and PdAg, 0-5 pores/cm^2.

Life tests are designed to evaluate the ability of the coating to function under various environmental or physical conditions. Battelle Class II FMG is a life test designed to promote failure due to porosity [12]. The pore density after exposure to Battelle Class II FMG more than likely reflects the porosity of the gold surface layer. For GFPdNi, the high level of porosity in the thin gold layer provides abundant sites for attack of the PdNi by the corrosive gasses. The thicker, less porous WE#1 layer affords more protection of the PdAg than the thinner AuCo provides PdNi.

FORMABILITY

Formability was evaluated using 90° V-blocks with radii ranging from 0.25 mm to 4.0 mm. Base metal samples were bent in order to determine the minimum bend radius for base metal initiated failure. The coated samples were then bent. The formed surface was subsequently exposed to nitric acid vapors as specified in ASTM 8-735 and visually examined to evaluate the surface continuity. The surface was considered contiguous if no Ni indications were detected at a magnification of 10x. The results are tabulated in Table III.

TABLE III: MINIMUM BEND RADIUS (MBR) AND R/T RATIO FOR C17410, WE#1/PdAg AND GFPdNi.

MATERIAL	MBR	R/T
C17410	.25 mm	1.0
WE#1/PdAg	1.0-1.3 mm	4.0-5.2
GFPdNi	3.5-4.0 mm	14.0-16.0

Given the base metal thickness, the coating thicknesses, the coating properties, and assuming 50 to 100 gram contact loads and crossed rods mating geometry, and using connector design guidelines published by Hobgood and Kantner, the Rlt ratio should be less than 6 to assure reliability [13]. The performance of GFPdNi mandates post form electroplating of stamped parts. On the other hand, WE#1/PdAg may be stamped and formed in a single die operation.

TEMPERATURE STABILITY

Figure 1 depicts contact resistance plotted versus aging time at 150°C for 80Pd20Ni and GFPdNi. The contact resistance of 80Pd20Ni rapidly increases within the first 50 hours. The initial rise is due to oxidation of the Ni. Subsequent increases are due to oxidation of Ni and/or Cu accumulating at the surface by diffusion. The gold flash attenuates the oxidation reaction, extending the useful life to somewhere between 500 and 800 hours.

Figure 2 depicts contact resistance plotted versus aging time at 150°C for 60Pd40Ag and WE#1/PdAg. The contact resistance of 60Pd40Ag increases from about 3.0·mΩ to about 10 mO after aging for 2000 hours.

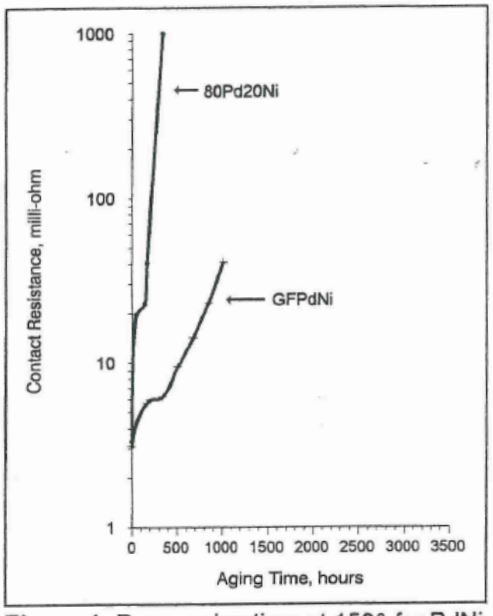

Figure 1. R_c vs. aging time at 150° for PdNi and GFPdNi.

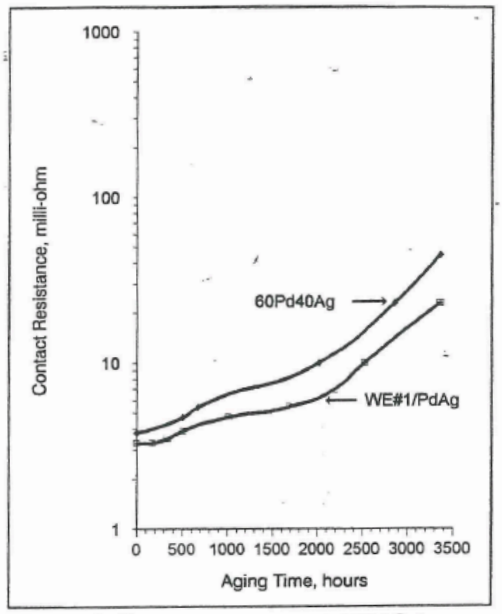

Figure 2. R_c vs. aging time at 150°C for PdAg and WE#1/PdAg.

The contact resistance of WE#1/PdAg increases to 10.0 mΩ after about 2500 hours. The cause of the contact resistance rise for both materials is Ni diffusion to the surface and subsequent oxidation. The difference in observed behavior for 80Pd20Ni and 60Pd40Ag and, GFPdNi and WE#1/PdAg is directly related to layer microstructure, constitution and thickness. Starting with the Ni diffusion barrier, Bitler postulated a grain size effect on the diffusivity of Cu through Ni diffusion barriers [14]. Lees confirmed that the diffusivity of Cu in electroplated Ni was significantly larger than the diffusivity of Cu in wrought Ni [15]. Using data published by Marx et a/ [16] and, Lees [15], at 150°C, about 11.0 µmeter of electroplated Ni would be required to prevent Cu from reaching the contact material in 3000 hours, while only 2.0 µmeter of wrought Ni would be an effective barrier [15,16]. The 2.0 µmeter thick electroplated Ni barrier specified for this study was ineffective in preventing Cu diffusion to and subsequent contamination of the contact surface. The,wrought barrier was sufficiently thick to prevent Cu diffusion.

The intermediate layer constitution also affects contact resistance behavior. In the previously cited study, Lees demonstrated that as the aging temperature approaches 180°C, diffusion of Ni from the barrier becomes the predominant failure mode [15]. Ni is completely miscible in Pd but not in PdAg. The limited solubility primarily affects bulk diffusion and influences grain boundary diffusion. The diffusivity of Ni in PdNi should be larger than that of Ni in PdAg.

In a separate study, Lees measured the diffusivity of Ni in 60Pd40Ag and found it to be lower than published diffusivities for Ni in Pd [17]. The contact resistance results after aging suggest that 60Pd40Ag is a better barrier to Ni diffusion than 80Pd20Ni.

BATTELLE CLASS II FMG

Figure 3 depicts a probability plot of contact resistance versus cumulative per-cent for GFPdNi coupons exposed to Battelle Class II flowing mixed gas for 0, 48, 96 and, 240 hours. A total of 100 measurements were obtained for each exposure. Note that the 0 exposure or, initial distribution, demonstrates a slight tail effect.

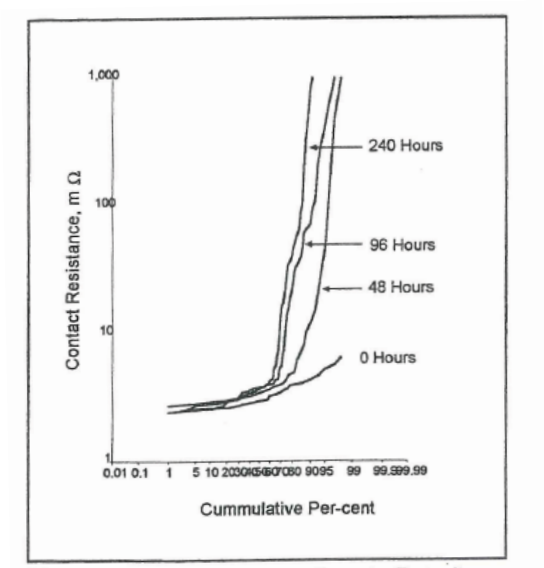

Figure 3. R_c vs. exposure time to Battelle Class II FMG for GFPdNi.

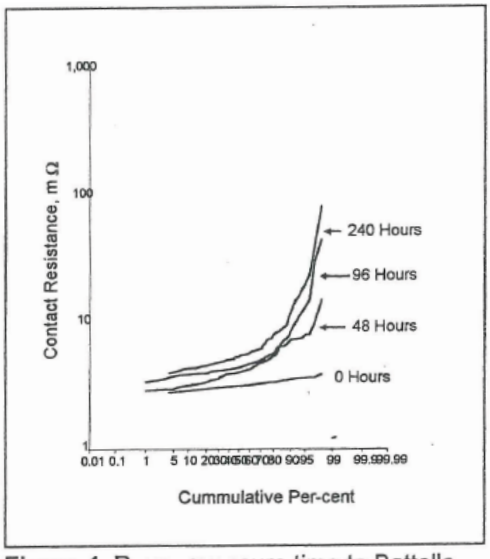

Figure 4. R_c vs. exposure time to Battelle Class II FMG for WE#1/PdAg.

After 48 hours more than 10 % of the readings were above 13 mΩ (ΔR = 10 mΩ). Increased exposure increased the number of readings above 13 mΩ. After 240 hours, more than 30 % of the readings exceeded this limit. Contact resistance values of 1 Ω for the 240 hour exposure.

Figure 4 depicts a probablitiy plot of contact resistance versus cumulative per-cent for WE#1/PdAg coupons exposed to Battelle Class II flowing mixed gas for 0, 48, 96 and 240 hours. A total of 100 measurements were obtained for each exposure. Note the slight increase in resistance level as exposure time increases. After 48 hours less than 5% of the readings were above 13 mΩ (ΔR = 10 mΩ).

Increased exposure increased the number of readings above 13 mΩ. After 240 hours, 10 % of the readings exceeded this limit which is significantly less than the 30% observed for GFPdNi. Maximum contact resistance values for exposure of 48, 96 and 240 hours were 15, 45 and 83 mΩ respectively.

The differences in the contact resistance distributions for GFPdNi and WE#1/PdAg may be attributed to the differences in the level of porosity of the surface layer. The gold flash may contain as many as 350 pores/cm^2; the WE#1 as few as 35. Pd, PdAg, and, PdNi are attacked by Cl_2 and NO_2 + SO_2 mixtures. These gasses are present in the Battelle Class II FMG. Corrosion resistance and therefore electrical stability, after exposure to this environment is a function of the integrity of the outer layer. The WE#1 is less porous and affords greater resistance to attack.

There are subtle differences between the two figures that suggest different corrosion processes. The GFPdNi exhibits almost bimodal behavior regardless of exposure time. For 48, 96 and, 240 hour exposures, the readings up to 50% are nearly identical and the distributions overlap. Beyond 50%, the distributions abruptly change but appear to parallel one another. On the other hand, the WE#1 distributions demonstrate a more continuous change after about the 80th percentile. Further, the distributions do not coincide and appear offset or stacked. Visual examination of the surfaces after exposure provided additional insight. The corrosion products on the surface of the GFPdNi are well-defined and intensify in color as exposure time increases. The surface appearance suggests localized film formation resulting in discrete areas of corrosion product on the gold surface. The bimodal nature of the distribution probably results from measuring both the contact resistance of gold and that of the corrosion product. Conversely, the corrosion products on the WE#1/PdAg surface were indistinct.

Subtle reflectivity changes were observed as exposure time increased., The contact resistance behavior and the observations suggest that a continuous film layer has formed on the surface. The corrosion film on the WE#1/PdAg surface required much longer exposure times to produce deleterious contact resistance changes than the discrete areas that formed on the GFPdNi surface. Further analysis is required to quantify these observations.

SLIDING WEAR

Figure 5 depicts coefficient of friction (COF) plotted versus number of wear cycles for GFPdNi sliding against GFPdNi at contact forces of 0.5 N through 10.0 N.

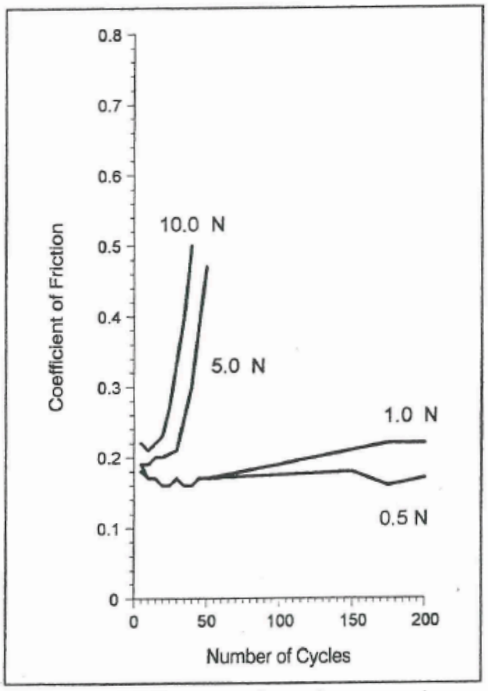

Figure 5. COF vs. number of wear cycles for GFPdNi mated with GFPdNi.

The results of three replicate runs were averaged to determine the COF values. A CQF value of 0.4 is a typical upper limit for both wear stability and insertion/withdrawal force specification. Based on the results, the electroplated system should be suitable for applications bounded by the following force-wear cycle conditions:

0.5 N: greater than 200 cycles, 1.0 N: greater than 200 cycles, 5.0 N: 45 cycles, and 10.0 N: 35 cycles.

Figure 6 depicts COF plotted versus number of wear cycles for WE#1/PdAg sliding against WE#1/PdAg at contact forces of 0.5 N through 10.0 N.

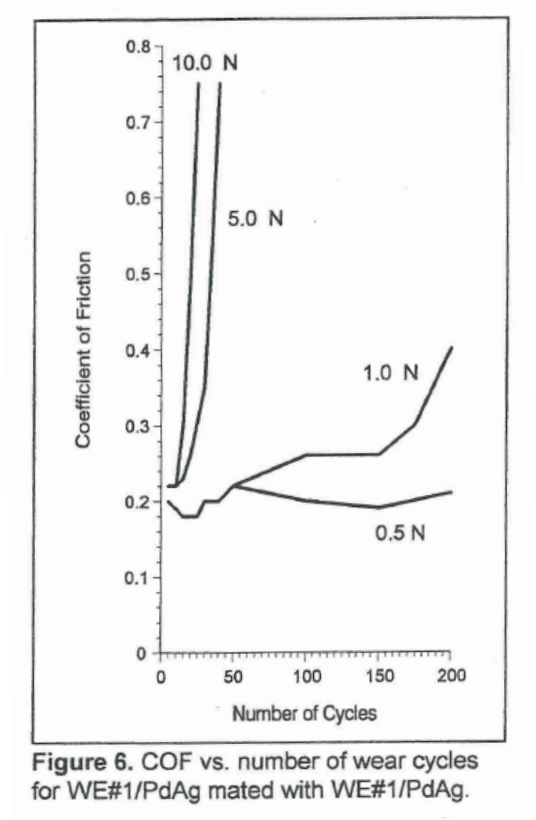

Figure 6. COF vs. number of wear cycles for WE#1/PdAg mated with WE#1/PdAg.

The results of three replicate runs were averaged to determine the COF values. Using the same criteria detailed above, the clad inlay contact system should be suitable for applications bounded by the following force-wear cycle conditions: 0.5 N: greater than 200 cycles, 1.0 N: greater than 200 cycles, 5.0 N: 30 cycles, and 10.0 N: 20 cycles.

At 0.05 N contact force, both GFPdNi and WE#1/PdAg demonstrated near identical behavior. The COF for the GFPdNi system was about 10% lower than that of the WE#1/PdAg system. At 1.0 N contact force, both systems demonstrated· acceptable behavior. COF for the WE#1/PdAg system began to rise after about 150·cycles, but was below 0.4 after 200 cycles. COF for the GFPdNi system remain essentially constant throughout the test. At higher loads, the number of wear cycles decreased. The GFPdNi system proved more durable. However, both systems could be successfully applied in high load applications where the number of insertion/withdrawal cycles is typically less than 10.

FRETTING

The statistical design of the fretting experiment was a classical 2x2x2x2 factorial design [18]. The test conditions are summarized in Appendix 1. In this type of design, one variable is fixed and all other variables changed. This system of testing allows the material system to be evaluated using all possible combinations of the other variables. Each of the 16 combinations was considered for statistical analysis purposes and permits testing specific conditions using the statistical technique of contrasts [19]. Each experimental condition was repeated 5 times to minimize mean squared error.

TABLE IV: SUMMARY OF THE RESULTS OF FRETTING WE#1/PdAg VS. WE#1/PdAg AND GFPdNi VS. GFPdNi. VALUES ARE CYCLES TO FAILURE.

TEST CONDITION	WE#1/PdAg	GFPdNi
Overall	92,343	14,416
40% RH	46,378	7,785
80% RH	138,310	21,048
10 mA current	121,547	17,087
100 mA current	63,142	10,844
20 µ-meter amplitude	124,542	18,358
50 µ-meter amplitude	60,236	10,474

The statistical analysis revealed that WE#1/PdAg versus WE#1/PdAg demonstrated the best performance under the these fretting conditions. Relative humidity, fret amplitude and level of current flowing through the contact were also significant. Contrast analysis yielded the following trends. Higher relative humidity, increased cycles to failure while both increased fret amplitude and current flow decreased cycles to failure.· The same trends were observed for GFPdNi. Table IV summarizes the results. The overall performance of the GFPdNi system mirrors the results of Whitlaw, Nobel and Morse [20-22]. GFPdNi has exhibited low fretting resistance under a variety of test conditions including fixed amplitude coupon studies and temperature cycling and vibration studies using specific connector designs. Failure

modes included fretting wear and frictional polymer formation.

The overall performance of the WE#1/PdAg system has been reported for components subjected to both temperature cycling and random vibration [11]. Those results indicated that this system was satisfactory for the specific experimental conditions.

These results summarize the first fixed amplitude coupon study of WE#1/PdAg. The results correlate with studies conducted by Antler on DG R156 mated with DG R156 [23]. In that study, unlubricated fretting of DG R156 versus DG R156 resulted in a contact resistance rise of about 20 mΩ between 10,000 and 100,000 cycles.

The influence of humidity on fretting performance can be explained as follows. Metals have adsorbed layers of gas on their surfaces [4]. One species of gas is water vapor. At low humidity levels the amount of adsorbed water will be low. As the relative humidity increases, the amount of adsorbed water increases. The water molecules probably act as a lubricant and decrease fretting wear.

The results of the current study indicate that increasing the fret amplitude decreases the cycles to failure and are consistent with prior studies. The influence of fret amplitude has been documented by Antler [24]. The amount of insulating film which is produced during fretting is dependent on the wipe distance. As the fret amplitude increases, the amount of insulating film increases.

The influence of current flow on fretting performance has been reported by Morse [22]. The application of 100 mA of current through the contact interface caused a 2:1 reduction in the number of cycles to failure for both GFPdNi and gold contact systems when compared to tests conducted with no current flow. The results in Table IV are consistent with that study; as current flow increased, cycles to failure decreased.

Surface examination provided insight into the difference in behavior of WE#1/PdAg and GFPdNi. The wear tracks were examined using an optical microscope at magnifications up to 500x. Wear debris, both within and at either end of the wear track, was a mixture of metallic particles and organic matter. GFPdNi versus GFPdNi debris consisted of metallic and organic particles. WE#1/PdAg versus WE#1/PdAg debris consisted of metallic particles, organic particles and organic films.

Abbott and Campbell studied frictional polymer formation and concluded that film type polymers formed on gold-gold interfaces after short induction periods. Much longer periods were required to produce particulate type polymers on palladium-palladium interfaces [5]. The observed wear debris mixtures suggest that for GFPdNi used in this study, the gold flash was rapidly removed, probably within the first several thousand cycles. The initial Au-Au interface was transformed to PdNi-PdNi through wear, and particulate frictional polymer formed. The particulate polymer reduces friction but causes contact resistance to increase.

The wear debris observed after fretting WE#1/PdAg versus WE#1/PdAg suggests that the WE#1-WE#1 interface was maintained for sufficient time to form film type polymer. Film polymers reduce friction and permit asperity contact. The presence of particulate polymer implies that, eventually the interface was transformed by wear to PdAg-PdAg, the particulate polymer formed and the contact resistance increased.

The implication of these observations is that if an Au-Au interface is maintained beyond the induction period for producing film type polymers, friction, and therefore wear will be reduced, and cycles to failure will increase.

CONCLUSIONS

HARDNESS AND ELECTRICAL RESISTIVITY

GFPdNi is harder than WE#1/PdAg. The electrical resistivity of AuCo and PdNi are lower than WE#1 and PdAg. This difference may be significant for those applications where total circuit resistance is important. The measured contact resistance of WE#1/PdAg was equivalent to that of GFPdNi.

POROSITY

The porosity of both WE#1/PdAg and GFPdNi are very low, less than 5 pores per square centimeter, when measured by a standard porosity test.

Significant differences appeared after GFPdNi and WE#1/PdAg were exposed for short periods of time to flowing mixed gas. The porosity of GFPdNi increased by an order of magnitude, while that of WE#1/PdAg remained unchanged.

FORMABILITY

The bend ductility of GFPdNi was inferior to that of WE#1/PdAg. In order to meet published guidelines for reliability, connector designs based on GFPdNi as a contact surface must be formed before the contact material is applied. If secondary die operations are required, additional tooling costs may be incurred. WE#1/PdAg, on the other hand, proved capable of being stamped and formed in a single die operation.

TEMPERATURE STABILITY

80Pd20Ni rapidly oxidized when aged in air at 150°C. Both Ni and Cu diffused to the contact surface. Over coating PdNi with a gold flash attenuated the process. However, electrical instability occurred between 500 and 800 hours.

The contact resistance of 60Pd40Ag began to degrade after about 2000 hours. WE#1/PdAg began to degrade after about 2500 hours.

The degradation of WE#1/PdAg was caused by Ni diffusion from the barrier material to the contact surface and the subsequent oxidation of the Ni. However, there was five-fold increase in time-to failure for WE#1/PdAg when compared to GFPdNi.

BATTELLE CLASS II FMG

The contact resistance of GFPdNi degraded rapidly after exposure to Battelle Class II FMG. After 48 hours, more than 10% of the readings exceeded a ΔR of 10 mΩ. After 240 hours, more than 30 % of the readings exceeded a ΔR of 10 mΩ. Maximum readings were in the 1Ω range.

The contact resistance of WE#1/PdAg degraded to a lesser degree. Less than 5 % of the readings exceeded a ΔR of 10 mΩ after 48 hours. After 240 hours, about 10% of the readings exceeded a ΔR of 10 mΩ. The maximum value measured was 83 mΩ.

SLIDING WEAR _

GFPdNi demonstrated better wear performance as measured by COF changes for loads ranging from 1.0 to 10.0 N. Both initial and stable COF values were typically 10% lower than those for WE#1/PdAg.

WE#1/PdAg demonstrated adequate performance at high and intermediate loads.

The performance of both material systems at low, 0.5 N, loads was indistinguishable.

FRETTING

GFPdNi exhibited low fretting resistance under a variety of test conditions including different levels of fret amplitude, current flow and, relative humidity. The AuCo-AuCo interface was rapidly transformed to PdNi PdNi by wear. The formation of deleterious particulate frictional polymers ensued and contact resistance increased.

WE#1/PdAg exhibited a six-fold increase in cycles-to-failure when compared to GFPdNi. The WE#1-WE#1 interface survived for sufficient time to permit the formation of film type frictional polymers. Lubrication of the interface attenuated the wear process thereby increasing cycles-to failure.

SUMMARY

WE#1/PdAg, which is a Materion iON connector material, exhibited ample hardness, low Rc, very low porosity, preferrred oxidation and corrosion resistance, better formability, acceptable durability, and superior fretting resistance when compared to GFPdNi.

REFERENCES

For technical data and experimental methods, please contact our team at 401.288.0690.

APPENDIX 1: A LIST OF THE FRETTING EXPERIMENTAL CONDITIONS.

RUN	MATERIAL SYSTEM	FRET AMPLITUDE, µ-METER	CURRENT FLOW, mA	RELATIVE HUMIDITY, PERCENT
1	WE#1/PdAg vs. WE#1/PdAg	20	10	40
2		50	10	40
3		20	100	40
4		50	100	40
5		20	10	80
6		50	10	80
7		20	100	80
8		50	100	80
9	GFPdNi vs. GFPdNi	20	10	40
10		50	10	40
11		20	100	40
12		50	100	40
13		20	10	80
14		50	10	80
15		20	100	80
16		50	100	80